# Manganoan fayalite and products of its alteration from the Strzegom pegmatites, Poland

J. JANECZEK

Department of Earth Sciences, Silesian University, Mielczarskiego 60, 41-200 Sosnowiec, Poland

**Abstract**

Nodules of manganoan fayalite occur in schlieren pegmatities in the vicinity of Strzegom, Lower Silesia. The fayalite, $Na_{0.02}(Fe^{2+}_{1.81}Mn_{0.16}Mg_{0.03})Si_{0.99}O_4$, is unzoned and non pleochroic. $2V_\alpha = 42°$, $a$ 4.826(3), $b$ 10.500(2), $c$ 6.102(2) Å, $d_{130obs.} = 2.83$ Å, $d_{130calc.} = 2.833$ Å, $D = 4.35\,g\,cm^{-3}$, $D_{calc.} = 4.353\,g\,cm^{-3}$. The role of $Na^+$ ions in the fayalite chemistry is discussed. The fayalite underwent multi-stage hydrothermal alteration beginning at the highest temperature (440 °C) of homogenization of gaseous-fluid inclusions in quartz adjacent to the fayalite grains. Increase in $f_{O_2}$ and then in $P_{H_2O}$ resulted in the formation of magnetite–quartz and Mn-grunerite–magnetite–quartz aggregates within the fayalite grains. The fayalite is mantled by a Mn-greenalite–magnetite rim, Mn-grunerite–magnetite–Mn-minnesotaite zone in a stilpnomelane or greenalite-rich groundmass. The minnesotaite is believed to have formed at the expense of grunerite. Stilpnomelane, the most abundant silicate phase in the rim, is the product of biotite and presumably greenalite alteration at the second stage of increasing Na activity (the crystallization of cleavelandite) in the pegmatites. The fayalite is also heavily altered to iddingsite—a composite mixture of amorphous FeOOH and silica. The iron-hydroxide recrystallized partially to poorly-crystalline goethite.

KEYWORDS: Mn-fayalite, pegmatite, Strzegom, Poland.

## Introduction

FOR many years the origin of 'limonite' pseudomorphs after a mysterious mineral that had occasionally been collected from pegmatites in two large granite quarries near Strzegom (pronounced Stch'egom) was unknown. Only recently the pre-existing mineral—manganoan faylite has been found together with a suite of secondary iron and manganese-rich phyllosilicates and amphibole.

*Occurrence.* Granite from the vicinity of Strzegom belongs to the Strzegom–Sobótka massif (Lower Silesia)—a composite intrusive body of a Variscean age (299–323 Ma), divided broadly into two parts separated by a regional fault. The western part of the massif, where the fayalite pegmatites occur, is a shallow, post-tectonic intrusion composed of biotite–hornblende granite partly surrounded by a fine-grained leucogranite. The eastern part of the massif represents a deeper level of the pluton and is built up of biotite granodiorite, two-mica leucogranite and minor bodies of tonalite (Majerowicz, 1972).

Miarolitic cavities yielding over 50 mineral species are ubiquitus in the biotite–hornblende granite (Janeczek, 1985). This suggests water-saturated conditions during emplacement.

Apart from the miarolitic cavities and aplite dykes, fayalite-bearing, flat-lying lenticular or sheet-like pegmatitic schlieren occur in the biotite–hornblende granite. They are unzoned, except for a transition zone a few centimetres wide of a fine-grained granite. Their width does not exceed 0.5 m. The pegmatites consist of maximum microcline perthite ($Or_{92}Ab_8$), albite ($Ab_{96-98}An_{0-1}Or_{1-4}$), quartz, iron-rich biotite, and fayalite. In tiny vugs cleavelandite, stilpnomelane, and stilbite have also been found. Idiomorphic microcline perthite is deep green when in contact with the fayalite and becomes creamish white when surrounded by iron-free minerals. Both microcline and quartz are heavily fractured. It should be emphasized that fayalite has not been found either in miarolitic cavities or in the granite and aplite.

*Fayalite.* The fayalite forms nodules up to 9 cm in diameter, anhedral against microcline. Unaltered fayalite is dark brown and its streak is grey. In thin section the fayalite is grey, yellowish or pale orange. No pleochroism was observed.

*Mineralogical Magazine, June 1989, Vol. 53, pp. 315–325*

Table 1. Representative microprobe analyses and structural formulae of manganoan fayalite and products of its alteration from the Strzegom pegmatites.

| | Fayalite | | | Grunerite | | | Greenalite | | | Minnesotaite |
|---|---|---|---|---|---|---|---|---|---|---|
| | J21 | J2B | J2BNS | J21 | J2B | J2BNS$^{X}$ | J2B | J2BNS | J2BNS$^{\delta}$ | J2BNS |
| $SiO_2$ | 29.55 | 29.36 | 29.63 | 48.23 | 48.02 | 48.33 | 36.30 | 36.75 | 36.41 | 49.50 |
| $Al_2O_3$ | 0.00 | 0.00 | 0.00 | 0.10 | 0.38 | 0.17 | 0.08 | 0.00 | 3.74 | 0.14 |
| FeO | 63.89 | 64.12 | 64.52 | 43.37 | 43.26 | 41.88 | 44.645 | 47.46 | 42.92 | 40.56 |
| MnO | 5.82 | 5.33 | 5.52 | 4.09 | 4.40 | 6.13 | 7.56 | 4.65 | 5.58 | 3.205 |
| MgO | 0.82 | 0.71 | 0.60 | 1.62 | 1.48 | 0.86 | 0.19 | 0.39 | 0.30 | 0.645 |
| CaO | 0.00 | 0.10 | 0.09 | 0.09 | 0.26 | 0.16 | 0.155 | 0.08 | 0.16 | 0.06 |
| $Na_2O$ | 0.22 | 0.45 | 0.32 | 0.29 | 0.425 | 0.21 | 0.285 | 0.30 | 0.13 | 0.15 |
| $K_2O$ | 0.00 | 0.00 | 0.00 | 0.00 | 0.00 | 0.00 | 0.00 | 0.00 | 0.62 | 0.07 |
| Total | 100.30 | 100.07 | 100.68 | 97.79 | 98.225 | 97.74 | 89.215 | 89.64 | 89.86 | 94.33 |
| | Structural Formulae Based on: | | | | | | | | | |
| | 4 oxygens | | | 23 oxygens | | | 14 oxygens | | | 11 oxygens |
| Si | 0.994 | 0.991 | 0.994 | 7.963 | 7.915 | 8.006 | 4.336 | 4.357 | 4.206 | 3.968 |
| $Al^{IV}$ | - | - | - | 0.019 | 0.074 | 0.000 | - | - | - | 0.014 |
| $Al^{VI}$ | - | - | - | - | - | 0.033 | 0.011 | - | 0.509 | - |
| $Fe^{2+}$ | 1.797 | 1.810 | 1.810 | 5.989 | 5.963 | 5.802 | 4.460 | 4.706 | 4.147 | 2.720 |
| Mn | 0.165 | 0.152 | 0.156 | 0.572 | 0.614 | 0.860 | 0.765 | 0.467 | 0.546 | 0.217 |
| Mg | 0.041 | 0.035 | 0.030 | 0.398 | 0.363 | 0.212 | 0.034 | 0.069 | 0.051 | 0.077 |
| Ca | - | 0.003 | 0.003 | 0.015 | 0.046 | 0.028 | 0.020 | 0.010 | 0.019 | 0.005 |
| Na | 0.014 | 0.029 | 0.020 | 0.136 | 0.135 | 0.067 | 0.066 | 0.034 | 0.029 | 0.024 |
| K | - | - | - | - | - | - | - | - | 0.092 | 0.007 |
| | | | | | | | 0.73 | 0.76 | 0.75 | |
| f | 0.98 | 0.98 | 0.98 | 0.94 | 0.95 | 0.97 | 0.99 | 0.99 | 0.99 | 0.97 |

J2BNS$^{X}$ - grunerite from the mantle
J2BNS$^{\delta}$ - admixtures of stilpnomelane are present in the sample
All microprobe analyses were made on a Cameca Camebax microprobe at the Geological Department of the University of Manchester. ZAF-4/FLS software was used for data reduction. Operating comditions: 15 kV accelerating potential, 40 deg take off angle, 3 nA beam current.

$2V_\alpha = 42°$. Unit cell parameters calculated from the X-ray powder pattern (Philips diffractometer, Cu-$K_\alpha$ radiation, Si internal standard) are: $a$ 4.826(3), $b$ 10.500(2), $c$ 6.102(2) Å, V 309.19(16) Å$^{-3}$, $d_{130obs.} = 2.829$ Å, $d_{130calc.} = 2.833$ Å. Density calculated on the basis of the unit cell dimensions $D_{calc.} = 4.353$ g cm$^{-3}$ is closely related to the density measured with a pycnometer $D_{meas.} = 4.35$ g cm$^{-3}$.

Microprobe data for the Strzegom fayalite together with analytical conditions are given in Table 1. The chemical composition of the fayalite is rather uniform throughout the grains although in some spots MnO concentration is as high as 7.7 wt.% causing an increase in the tephroite molecule up to $Te_{11}$.

Because of the small amount of Mg, the fayalite may be considered as belonging to the Fe–Mn binary. Therefore, it is possible to make use of the determinative diagrams of Miller and Ribbe (1985) to estimate the Fe and Mn distribution between $M1$ and $M2$ sites in the olivine structure. As it might be expected $Mn^{2+}$ ions are principally located in the $M2$ sites ($X_{Fe}^{M2} = 0.85$, $X_{Mn}^{M2} = 0.13$, $X_{Fe}^{M1} = 0.95$). Similar results were obtained using the plot of Annersten *et al.* (1984) ($X_{Fe}^{M2} = 0.84$).

## Alteration products

Alteration of the fayalite and biotite gave way to two groups of secondary minerals easy distinguishable by their chemistry (Tables 1 and 2, Figs. 1 and 2).

The Mn-fayalite underwent multi-stage alterations. Products of these alterations can be divided into internal assemblage, i.e. related to the breakdown of the olivine structure and occurring within the olivine grains, and external reac-

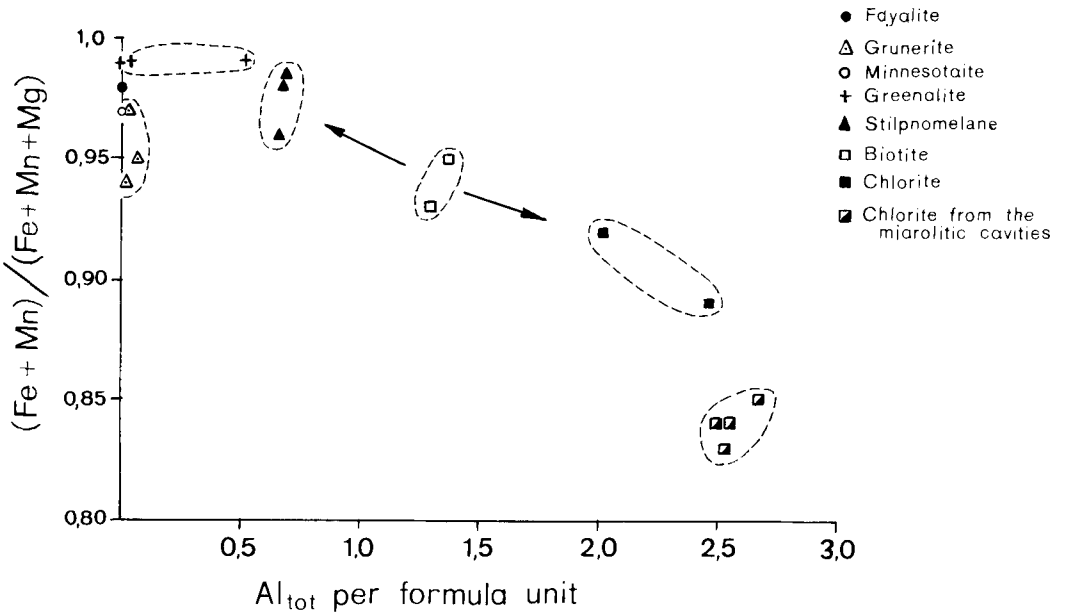


FIG. 1. (Fe + Mn)/(Fe + Mn + Mg) *vs.* Al atoms per formula unit of mafic minerals from the Strzegom fayalite pegmatite. Composition of chlorite from the miarolitic cavities are plotted for comparison.

tional assemblage forming a black mantle around the olivine. The first group includes quartz + magnetite, and grunerite + magnetite ± quartz aggregates as well as iddingsite. The mantle is zoned and the following zones can be roughly established outward from the fayalite (Fig. 3*a*): 1. the narrow (0.25 mm) rim of greenalite and magnetite contouring the fayalite grain boundary; 2. grunerite–magnetite–minnesotaite ± quartz aggregates surrounded by the groundmass of fine-grained, intimately intergrown iron-rich phyllosilicates, e.g. stilpnomelane; 3. stilpnomelane–chlorite zone developed at the expense of biotite.

*Grunerite.* Sheaf-like aggregates of grunerite associated with magnetite and quartz are abundant within the fayalite (Fig. 3*b*). In the black mantle, grunerite generally occurs in the form of fibrous radiating aggregates with relatively large idiomorphic magnetite grains at their centres (Fig. 3*c*). The area occupied by the grunerite–magnetite aggregates in the black mantle is larger than that of their counterparts from the interior of the fayalite grains, though the maximum length of the grunerite individuals is in both cases similar. However, while strongest peaks of grunerite are always present in the X-ray patterns of the Strzegom fayalite, especially when the magnetic fraction is analysed, they are absent from the X-ray patterns of the mantle. Therefore, it may be concluded that the quantitative contribution of the grunerite to the bulk composition of the mantle is lower than that of stilpnomelane, minnesotaite, and greenalite, whose peaks are always present in the X-ray patterns. On the other hand this may also indicate the uneven distribution of the grunerite within the mantle.

The chemical compositions of both grunerites are similar (Table 1). The main, but not striking, difference is a higher MnO concentration and lower MgO in the mantle grunerite. This is illustrated by the cummingtonite to dannemorite (Mn end-member of the grunerite–cummingtonite solid-solution series) molecular ratio which ranges from 0.66 to 0.87 for grunerite from the fayalite and is equal 0.33 for the mantle grunerite.

*Greenalite.* As is the case in greenalites from many iron formations, the Strzegom greenlite has more Si and less octahedral cations than its theoretical formula (Table 1, compare for instance with data in Floran and Papike, 1975). An explanation for Si excess and octahedral cation deficiency has been offered by Guggenheim *et al.* (1982). Greenalite is the most manganiferous product of fayalite alteration (Fig. 2). The symmetrical distribution of the greenalite and iddingsite in terms of their iron and manganese contents over the fayalite composition is noticeable (Fig. 2).

The caryopilite molecule content (caryopilite is a Mn analogue of greenalite) in the greenalite ranges from 8.9 to 14.5%. A similar content of

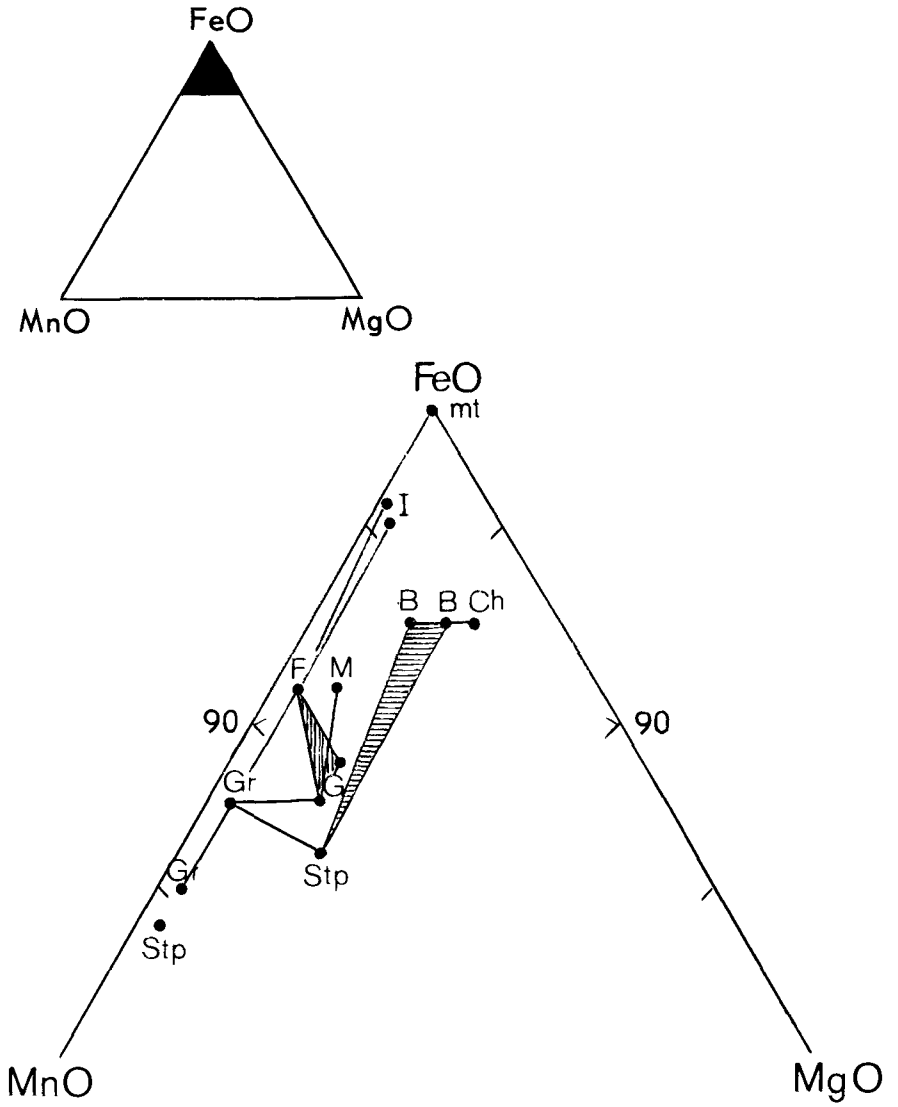


FIG. 2. Paragenetic FeO–MnO–MgO diagram for mafic minerals from the Strzegom fayalite pegmatite. B—biotite, Ch—chlorite, F—fayalite, G—grunerite, Gr—greenalite, M—minnesotaite, mt—magnetite, I—iddingsite, Stp—stilpnomelane.

MnO has been recorded for tosalite (Guggenheim *et al.*, op. cit.); however, the Strzegom greenalite has very low Al except for the J2BN sample, the microprobe analysis of which is suspect; the presence of some $K_2O$ in the latter suggests an admixture of stilpnomelane.

*Minnesotaite.* This mineral occurs as a fine-grained, high-birefringent substance adjacent to the grunerite–magnetite aggregates on one side and to the greenalite on the other. It was extremely difficult to obtain reliable microprobe data for the minnesotaite because of its intimate intergrowth with other constituents of the black mantle. Therefore, only one average representative electron probe analysis is presented (Table 1). The chemical composition of the Strzegom minnesotaite differs substantially from minnesotaite of metamorphic iron formations. Not only is the value of Fe/(Fe + Mg) ratio higher for the Strzegom sample but it is also the most Mn-rich phase.

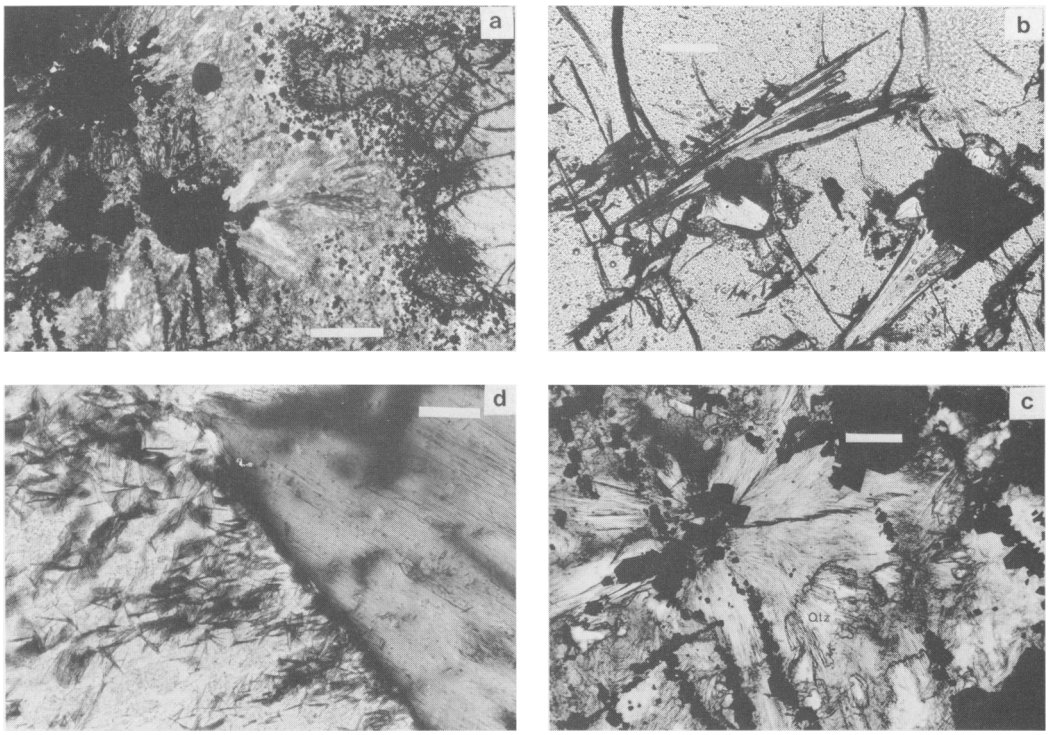


FIG. 3. (*a*) The 'black mantle' surrounding the Mn-fayalite grain. The irregular grain boundary is contoured by a Mn-greenalite–magnetite rim. The magnetite(black)–grunerite aggregates are immersed in the grunerite–minnesoatite background. Crossed polars. Scale bar = 0.5 mm. (*b*) Mn-grunerite–magnetite–quartz aggregates in the Mn-fayalite grain. Plane polarized light. Scale bar = 0.1 mm. (*c*) Radial aggregates of fibrous grunerite partially replaced by quartz (Qtz). Idiomorphic magnetite occurs at the centre of the aggregates and fills up the system of fractures. Plane polarized light. Scale bar = 0.2 mm. (*d*) Biotite altered at the margins to stilpnomelane. Plane polarized light. Scale bar = 0.1 mm.

*Stilpnomelane.* This is a common mineral in the Strzegom miarolitic cavities, where it has been described as an alteration product of Fe-chlorite (Sachanbiński and Janeczek, 1977). Curiously, this mineral was not recognized in the Strzegom samples by its discoverer Glocker who designated specimens he collected as 'glimmer?'. Both $Fe^{2+}$ and $Fe^{3+}$ varieties occur at the Strzegom locality, ferrostilpnomelane being predominant.

In the fayalite pegmatites stilpnomelane occurs as an alteration product of biotite (Fig. 3*d*) as well as the chief constituent of the groundmass. In thin section it is brown and displays pronounced pleochroism, from golden brown to dark brown, suggesting some content of $Fe^{3+}$. On the other hand, X-ray data ($d_{001}$ = 12.12 Å) and thermal behaviour point to ferrostilpnomelane.

Stilpnomelane and greenalite are the most manganiferous phases in the pegmatitic environment (Table 2, Fig. 2). Stilpnomelane concentrates Fe and Mn more effectively than the stilpnomelane in the miarolitic cavities. It is a compositional link between Al-free, fayalite-related assemblage and the biotite–chlorite group minerals (Fig. 1).

*The groundmass.* Fine grained groundmass, brown or green in colour, occurs among idiomorphic magnetite within the black mantle. Microprobe data for the groundmass are rather ambiguous (Table 3). Considerable variation of the totals at points separated from one another by a few microns seems to indicate a significant inhomogenity of the analysed material. Some of the analyses are closely related to stilpnomelane (high silica and potassium contents) regardless of their low Al content (analyses 1, 3, and 5 in Table 3). The others resemble the composition of greenalite. There is a third group of analyses in which silica is in excess and aluminium is absent, presumably reflecting the presence of quartz or amorphous silica (analysis 6 in Table 3).

Table 2. Representative microprobe analyses of biotite-related phyllosilicates from the fayalite-bearing pegmatite from Strzegom.

| | Biotite | | Chlorite | | Stilpnomelane | | |
|---|---|---|---|---|---|---|---|
| | J2B | J2BNS | J2B | J2BNS | J2B | J2BNS | J2B2 |
| $SiO_2$ | 32.23 | 33.36 | 24.69 | 24.705 | 42.29 | 42.83 | 42.51 |
| $Al_2O_3$ | 13.38 | 13.00 | 16.78 | 18.365 | 6.56 | 6.81 | 7.04 |
| FeO | 37.67 | 39.29 | 43.83 | 42.38 | 33.21 | 30.20 | 31.975 |
| MnO | 1.66 | 1.34 | 1.53 | 1.12 | 4.35 | 4.48 | 5.65 |
| MgO | 1.08 | 1.66 | 1.88 | 2.90 | 0.84 | 0.35 | 0.32 |
| CaO | 0.00 | 0.10 | 0.15 | 0.03 | 0.31 | 0.59 | 0.22 |
| $Na_2O$ | 0.26 | 0.35 | 0.27 | 0.38 | 0.19 | 0.29 | 0.36 |
| $K_2O$ | 7.04 | 6.86 | 0.00 | 0.04 | 2.00 | 2.35 | 1.77 |
| Total | 93.32 | 95.96 | 89.14 | 89.92 | 89.75 | 89.00 | 89.845 |
| | Structural Formulae Based on: | | | | | | |
| | 11 oxygens | | 14 oxygens | | 11 oxygens | | |
| Si | 2.783 | 2.801 | 3.170 | 2.811 | 3.560 | 3.607 | 3.5645 |
| $Al^{IV}$ | 1.217 | 1.199 | 0.830 | 1.189 | 0.440 | 0.393 | 0.4355 |
| $Al^{VI}$ | 0.145 | 0.088 | 1.195 | 1.274 | 0.211 | 0.283 | 0.2605 |
| $Fe^{2+}$ | 2.721 | 2.759 | 4.045 | 4.033 | 2.338 | 2.127 | 2.242 |
| Mn | 0.121 | 0.095 | 0.164 | 0.108 | 0.310 | 0.398 | 0.401 |
| Mg | 0.139 | 0.208 | 0.360 | 0.492 | 0.105 | 0.044 | 0.040 |
| Ca | 0.000 | 0.010 | 0.021 | 0.004 | 0.028 | 0.053 | 0.020 |
| Na | 0.043 | 0.057 | 0.067 | 0.084 | 0.031 | 0.047 | 0.058 |
| K | 0.776 | 0.735 | 0.000 | 0.006 | 0.215 | 0.252 | 0.189 |
| $\frac{Fe+Mn}{Fe+Mn+Mg}$ | 0.95 | 0.93 | 0.92 | 0.89 | 0.96 | 0.98 | 0.985 |

Table 3. Microprobe analyses of groundmass mantling Mn-fayalite in the Strzegom pegmatites.

| | 1 | 2 | 3 | 4 | 5 | 6 |
|---|---|---|---|---|---|---|
| $SiO_2$ | 45.29 | 37.02 | 43.90 | 52.88 | 42.84 | 68.46 |
| $Al_2O_3$ | 3.32 | 0.55 | 4.04 | 0.00 | 3.34 | 0.00 |
| FeO | 37.17 | 46.77 | 37.09 | 28.84 | 35.49 | 19.66 |
| MnO | 5.41 | 7.25 | 4.01 | 5.34 | 4.85 | 5.04 |
| MgO | 0.47 | 0.38 | 0.57 | 1.05 | 0.45 | 0.55 |
| CaO | 0.10 | 0.21 | 0.13 | 0.52 | 0.07 | 0.74 |
| $Na_2O$ | 0.51 | 0.49 | 0.02 | 0.33 | 0.43 | 0.00 |
| $K_2O$ | 2.45 | 0.00 | 2.63 | 0.35 | 2.37 | 0.00 |
| Total | 94.72 | 92.67 | 92.39 | 89.31 | 89.84 | 94.45 |

1 = brown groundmass adjacent to sphalerite. J2B sample; 2 = green groundmass close to iddingsite. J2B sample; 3 = green groundmass (see fig. 7); 4 = brown groundmass. J2B1 sample; 5 = brown groundmass. J2B sample; 6 = brown groundmass. J2B1 sample;

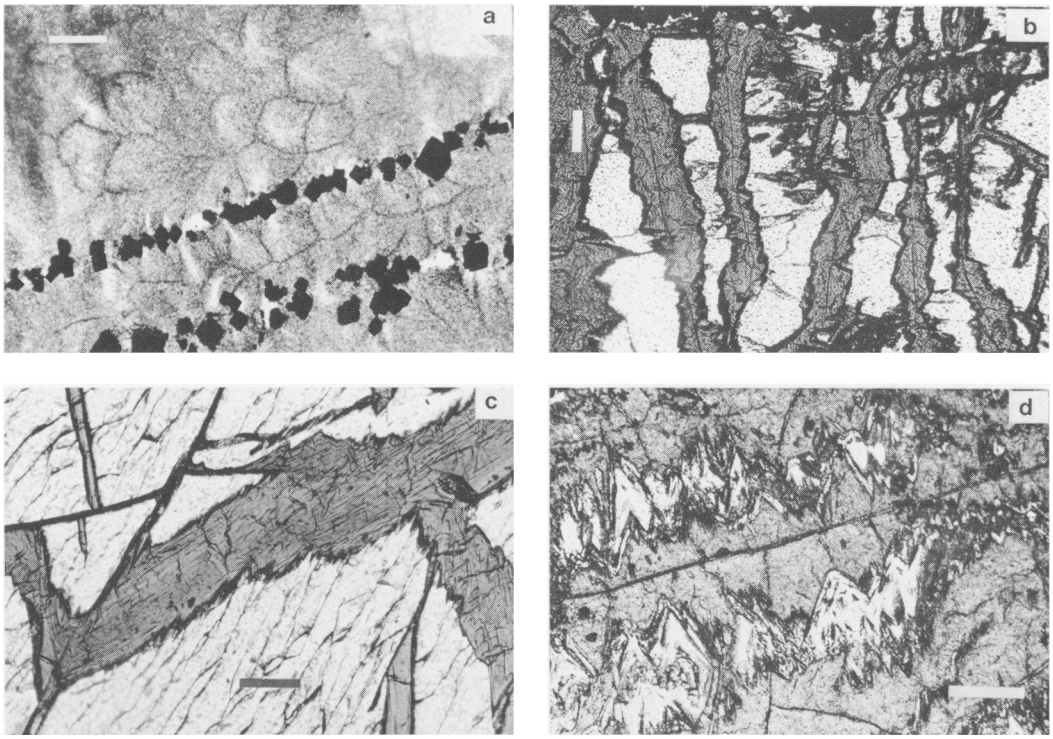


FIG. 4. (*a*) Stilpnomelane-rich green groundmass displaying a polygonal structure (for microprobe data see analysis 3 in Table 3). Margins of the polygons are enriched in magnetite. Note two parallel fractures filled with idiomorphic magnetite. Plane polarized light. Scale bar = 0.1 mm. (*b*) Iddingsite replacing Mn-fayalite along the system of fractures. Plane polarized light. Scale bar = 0.1 mm. (*c*) Internal structure of the iddingsite. Note a prominent (010) cleavage in the olivine. Plane polarized light. Scale bar = 0.1 mm. (*d*) Iddingsite (grey) alternating with silica (quartz + trydymite?) bands. The shark-teeth-like shape of the silica bands is the negative copy of the shape of the iddingsite 'rods'. Note the fracture symmetrically divided the 'rod' into two opposite directed parts. Plane polarized light. Scale bar = 0.2 mm.

X-ray powder diffraction analyses of the black mantle revealed the presence of stilpnomelane, greenalite, magnetite, and minnesotaite. Therefore, it may be concluded that the green groundmass that occurs at the contact with iddingsite is chiefly composed of stilpnomelane and greenalite intergrown with magnetite and amorphous (?) silica (Fig. 4*a*). The brown groundmass occurring closer to biotite consists predominantly of stilpnomelane. Minnesotaite is a minor but permanent constituent of both varieties of the groundmass. Moreover, a few grains of iron sphalerite and fluorite have been found as accessory constituents of the groundmass.

High-temperature X-ray analysis of the groundmass containing stilpnomelane, minnesotaite, and magnetite was performed using the DRON-2 diffractometer with the high-temperature attachment (Co-$K_\alpha$ radiation, Fe filter). A shift of the $d_{001}$ spacing was observed at high temperature (Fig. 5). The results for stilpnomelane are generally consistent with data provided by Eggleton (1972). The maximum $d_{001}$ value of 12.37 Å related to the $Fe^{2+}$ oxidation is very close to the $d_{001}$ of the extreme ferristilpnomelane of Eggleton and Chappel (1978). As temperature increases, a 'shrinkage' of the stilpnomelane structure is observed, finally leading to the collapse of the structure between 800 and 830 °C.

High-temperature behaviour of the minnesotaite is slightly different from that of the stilpnomelane (Fig. 5). The greatest expansion of its structure takes place at 750 °C, presumably also due to oxidation of ferrous iron, followed by rapid breakdown of the mineral. This is in agreement with the DTA study of Blake (1965) who concluded that the water is lost in minnesotaite from 600 to 750 °C.

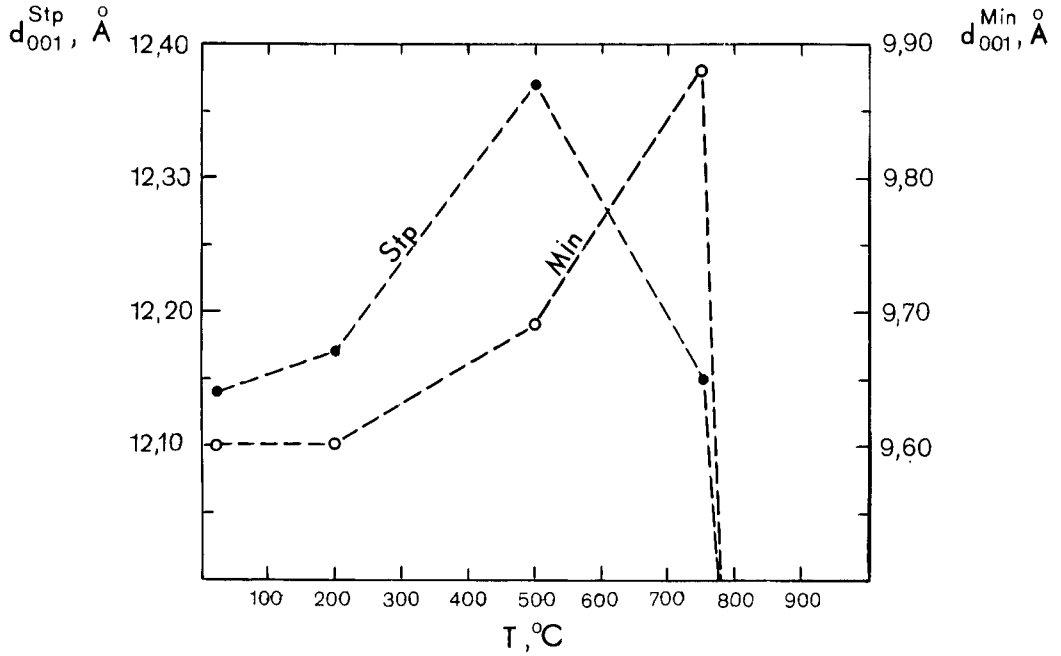


FIG. 5. Plot of $d_{001}$ against temperature for stilpnomelane (Stp—solid dots) and minnesotaite (Min—open circles) from the mantle.

*Iddingsite.* Almost all fayalite grains found in the Strzegom pegmatites are partly or entirely altered to reddish brown or brown iddingsite (Fig. 4*b*). Iddingsite commonly behaves optically as a homogenous substance (Deer *et al.*, 1982). However, in the case of the Strzegom samples, this is not so. Though isotropic, under crossed polars it displays bright streaks emphasizing the characteristic zig-zag pattern of its internal structure (Fig. 4*c*). In some samples, relatively wide silica bands alternate with iddingsite (Fig. 4*d*).

Complex pseudomorphs after fayalite composed of an orange–brown core surrounded by a dark brown rim are frequently found in the pegmatites. The rim is brittle, showing conchoidal fracture. It consists of an X-ray amorphous substance, magnetite, and quartz. The DTA curve of the amorphous phase displays two endothermic peaks. The very broad, low-temperature peak is attributed to the presence of molecular water, while the second peak at 310 °C is typical for goethite (conversion of $\alpha$-FeOOH to hematite). The core is predominantly built up of poorly crystalline goethite (or hydrogoethite), which formed due to recrystallization of the amorphous iron hydroxide. This is similar to the case described by Baker and Haggerty (1967), although the hydrothermal reheating described by these authors may not necessarily be involved in the process. The simple mechanism of 'ageing' of the gel-like iron hydroxide explains the formation of goethite. Otherwise it would be difficult to give a reason why crystalline goethite is covered by an amorphous substance.

The amorphous state of the primary iddingsite was confirmed by the X-ray diffraction analysis of the iddingsite adjacent to the unaltered fayalite. The only peaks in the X-ray pattern are those of grunerite, magnetite, and quartz. It is interesting to note that the grunerite is not susceptible to alteration to iddingsite.

The chemical composition of the iddingsite does not vary very much from sample to sample (Table 4). The $SiO_2$ content is very close to the average value for this substance (cf. Table 8 in Deer *et al.*, 1982). Manganese apparently plays the role of magnesium in basaltic iddingsites. When compared with Mn-fayalite, the iddingsite is relatively enriched in iron ($K_D = 1.88$ for total iron calculated as FeO), while the partition coefficient for manganese ($K_D = 0.31$) indicates that this element was released from the olivine structure during the alteration. The $K_D$ for magnesium is equal to unity.

Assuming that all silica in the microprobe analysis of the iddingsite is due to the presence

Table 4. Representative microprobe analyses of iddingsite from the fayalite-bearing pegmatite from Strzegom.

| | J2 | J2B | J2BNS | J2BNS |
|---|---|---|---|---|
| $SiO_2$ | 41.73 | 42.12 | 39.80 | 40.54 |
| $Al_2O_3$ | 0.00 | 0.00 | 0.00 | 0.00 |
| FeO | 38.29 | 38.99 | 37.68 | 37.73 |
| $Fe_2O_3^X$ | 42.55 | 43.33 | 41.875 | 41.93 |
| MnO | 1.405 | 1.17 | 1.16 | 1.06 |
| MgO | 0.24 | 0.19 | 0.21 | 0.23 |
| CaO | 0.75 | 0.64 | 0.73 | 0.76 |
| $Na_2O$ | 0.255 | 0.59 | 0.39 | 0.41 |
| $K_2O$ | 0.00 | 0.04 | 0.00 | 0.13 |
| Total | 82.57 | 83.74 | 79.97 | 80.86 |
| Total$^{XX}$ | 86.83 | 88.08 | 84.165 | 85.06 |

$^X Fe_2O_3$ calculated from the total Fe reported in the microprobe analyses as FeO

$^{XX}$Total related to the total iron reported as $Fe_2O_3$

of a separate silica phase (quartz or amorphous silica), it is possible to recalculate the analysis (J2BNS sample has been taken as an example) to obtain the chemical composition of a 'pure' hydroxide. This leads to the following formula calculated relative to 3 oxygens:

$$(Fe^{3+}_{1.901}Mn_{0.058}Mg_{0.016}Ca_{0.040}Na_{0.033}K_{0.001})_{\Sigma 2.048}O_3.$$

## Discussion

Textural observations suggest that manganoan fayalite in the Strzegom pegmatites crystallized after K-feldspar and prior to biotite, at an $f_{O_2}$ close to that of the QFM buffer as indicated by the adjacent quartz–magnetite aggregates within the fayalite. The general appearance of the pegmatites i.e. schlieren-like shape, and their gradational transition into the surrounding granite, suggests that the temperature interval for fayalite crystallization was that of 'normal' pegmatite crystallization, i.e. 600–500 °C. The abundance of miarolitic cavities, widespread low-temperature hydrothermal activity and other petrologic evidence (Majerowicz, 1972; Puziewicz, 1985) are characteristic of shallow-level intrusions. Thus, the total consolidation pressure may have not been higher than 1–2 kbar (3–5 km depth).

Numerous tiny gaseous-fluid inclusions are observed in quartz adjacent to the fayalite. Most of them are secondary inclusions grouped into several linear systems apparently related to more or less effectively healed fractures. They cover quite a large range of temperatures of homogenization ($T_H$) from 120 to 300 °C. There are also solitary inclusions with the volumetrically significant role of the gaseous phase that show $T_H$ with two maxima at 380–370 and 440 °C. The higher temperature presumably reflects the beginning of subsolidous alteration, whereas the lower temperatures coincide with the temperature range of albitization in the Strzegom pegmatites that was estimated as 400–300 °C (Nowakowski and Kozłowski, 1983).

Possible reactions that led to hydrothermal alteration of the fayalite are most probably the same as those that have been deduced from mineral assemblages of metamorphic iron-formations (see for instance Klein, 1974; Floran and Papike, 1975; Miyano and Klein, 1983).

Increase in $P_{H_2O}$ resulted in the breakdown of fayalite and the formation of the Mn-grunerite–magnetite–quartz aggregates through the following reaction (using composition data for the J2BNS sample from Table 1):

$$9.5\ \text{Fayalite} + 3.H_2O = \text{Mn-grunerite} + 1.4\ \text{Quartz} + 3.8\ \text{Magnetite} + 0.7\ Mn^{2+} + 0.1\ Mg^{2+} + 2H_2.$$

Outside the fayalite grains, the reaction could proceed as follows:

$$8\ \text{Fayalite} + 3.6\ H_2O = \text{Mn-grunerite} + 2.9\ \text{Magnetite} + 0.4\ Mn^{2+} + 2.6\ H_2.$$

From these reactions it is clear that the alteration process requires only the addition of $H_2O$.

The intensive fracturing of the pegmatites, easily observed even in hand-specimens, played an important role in the alteration process, enabling solutions to penetrate the fayalite. At least three fracture systems can be recognized in the samples studied (Figs. 3*a* and 4*a*).

As it was shown by Wones and Gilbert (1969), fayalite is not stable in the presence of aqueous phase below 250 °C and decomposes to magnetite and greenalite, this process took place in the Strzegom pegmatites. The upper stability limit for greenalite is at approximately 470 °C. The greenalite–magnetite rim adjacent to the fayalite grains may have formed through the reaction:

$$3(Fe, Mn)_2SiO_4 + 3H_2O = (Fe, Mn)Si_2O_5(OH)_4 + Fe_3O_4 + SiO_2 + H_2.$$

Since the greenalite–magnetite rim is deficient in silica, one may conclude that the excess silica partially replaced the grunerite. It may have also been consumed in the reaction:

$$3\ \text{grunerite} + 4SiO_2 + 4H_2O = 7\ \text{minnesotaite}.$$

Textural observations, although not unequivocal, suggest that minnesoatite is the product of grunerite alteration rather than fayalite. Forbes (1977) has proposed the temperature range of 270 to 300 °C (1–2 kbar $P_{H_2O}$) for the production of grunerite through the decomposition of minnesotaite. The upper stability limit of minnesotaite was calculated to be 310 °C and 1 kbar (Miyano and Klein, 1983).

So far only $Fe^{2+}$-bearing phases have been considered, suggesting reducing conditions close to the QFM buffer during hydrothermal alteration of fayalite. In some pegmatites, however, substantial amounts of $Fe^{3+}$ are incorporated into the fayalite structure, e.g. in ferri-fayalite from Uzbekhistan (Ginzburg *et al.*, 1961). Although nothing conclusive can be said about the valence state of iron in the Strzegom fayalite, the consistent presence of sodium in microprobe analyses is striking, suggesting the $Fe^{2+}\ Na^{+} \rightleftharpoons Fe^{3+}$ substitution. Thus, the formula of the fayalite could also be written:

$$Na_{0.02}(Fe^{2+}_{1.77}Fe^{3+}_{0.02}Mn_{0.16}Mg_{0.03})_{\Sigma 1.98}Si_{0.99}O_4.$$

Sodium, though in minor amounts, is present in all the mafic minerals, marking its high activity in hydrothermal solutions. It was the process of albitization that made biotite unstable in drusy cavities (Janeczek, 1985) and presumably in the pegmatites.

In the fayalite pegmatites, biotite grains are partially converted to chlorite. These grains are composed of alternating layers of dark green chlorite and pale green biotite. Assuming that Al is conserved, the following reaction accounts for the biotite chloritization (minerals composition data in Table 2):

$$1.91\text{Biotite} + 0.31Mn^{2+} + 0.09Mg^{2+} + 5.24H_2O + 1.93H_2 = \text{Chlorite} + 1.39K^{+} + 0.03Na^{+} + 0.02Ca^{2+} + 1.25Fe^{2+} + 2.54H_4SiO_4.$$

Titanium content in the biotite is below the detection limit of the microprobe. Therefore, titanite or ilmenite, common chloritization products, do not occur in the Strzegom samples.

High $Na^{+}$ ion activity favours the formation of stilpnomelane. In drusy cavities, stilpnomelane is associated with cleavelandite and, sometimes, with schorl. The temperature range for cleavelandite crystallization has been evaluated from a fluid inclusions study to be 300 to 130 °C (Nowakowski and Kozłowski, 1983). Formation of the schorl ranged from 255 to 155 °C (Lenkowski, 1983). Stilpnomelane associated with cleavelandite occurs in tiny vugs that formed due to dissolution of K-feldspar in the fayalite pegmatite. Therefore, by analogy, it may be concluded that biotite altered to stilpnomelane in the pegmatites at the stage of cleavelandite crystallization during the replacement reaction (based on mineral composition data for J2BNS sample in Table 2 and on the conservation of Al):

$$0.525\text{Biotite} + 0.68Fe^{2+} + 0.35Mn^{2+} + 0.02Na^{+} + 0.04Ca^{2+} = \text{Stilpnomelane} + 0.13K^{+} + 0.065Mg^{2+}.$$

This reaction has been written on the basis of the anhydrous formulae of the minerals. Otherwise, some $H_2O$ should be added to the left side of the equation.

Stilpnomelane presumably formed also by alteration of greenalite and possibly minnesotaite. Both minerals convert easily to stilpnomelane through the reactions (ignoring the zeolitic water in the stilpnomelane formula):

$$\underset{\text{Biotite}}{K(Fe, Mg, Mn)_3(Al, Si_3O_{10})(OH)_2} + \underset{\text{Greenalite}}{2Fe_3Si_2O_5(OH)_4} + SiO_2 = \underset{\text{Stilpnomelane}}{K_{0.6}(Fe, Mn, Mg)_6(Si_8AlO_{20})(OH)_4} + \underset{\text{Magnetite}}{Fe_3O_4} + 0.4K^{+}$$

$$\underset{\text{Biotite}}{K(Fe, Mg, Mn)_3(Al, Si_3O_{10})(OH)_2} + \underset{\text{Minnesotaite}}{(Fe, Mn)_3Si_4O_{10}(OH)_2} + SiO_2 = \underset{\text{Stilpnomelane}}{K_{0.6}(Fe, Mn, Mg)_6(AlSi_8O_{20})(OH)_4} + 0.4K^{+} + O_2.$$

These reactions, or reactions involving feldspars as reactants, probably account for the abundance of stilpnomelane in the mantle close to the biotite and alkali feldspars.

A similar alteration path has been described from pegmatites of the Cape Ann granite, Massachusetts (Wones and Gilbert, 1982). However, grunerite is thought to react there with perthite to produce annite, and at lower temperature, stilpnomelane. In the Strzegom pegmatites there is a lack of evidence for such reactions. It can be mentioned here that stilpnomelane replacing manganoan hastingsitic hornblende was found in other Strzegom pegmatites.

Formation of iddingsite from the Strzegom fayalite was caused by an increase of $f_{O_2}$ at the later stages of the hydrothermal activity. According to Frish (1972) iron knebelite in nordmarkite from Quebec was replaced by iddingsite prior to the formation of a clinopyroxene or amphibole

mantle surrounding the iddingsite. This concept cannot be applied to the Strzegom iddingsite. First, the problem of alteration of the mineral rimmed by others may be easily overcome if one takes into account the process of diffusion or percolation through porous or fractured surroundings. Moreover, olivine is extremely susceptible to any kind of alteration be it hydrothermal or weathering, whereas amphibole or pyroxene are relatively stable. This can be illustrated by the presence of unaltered grunerite within the iddingsite. What is more important, however, is the evolution of oxygen fugacity in the Strzegom pegmatites. A sufficiently high value of $f_{O_2}$ necessary to form iron hydroxide seems to be achieved at the stage of low-temperature zeolite crystallization or even later. The only occurrence of ferristilpnomelane in the Strzegon locality is restricted to those cavities that contain red chabazite contaminated with $Fe_2O_3$ up to 4.5 wt.% (Janeczek, 1985).

Iddingsitization of the fayalite started at grain boundaries working in towards the centres of the grains or sub-grains by making use of fractures that cross-cut the whole sample. Intersection of these fractures at right angles to the (010) fayalite cleavage, and with some other randomly oriented fractures, resulted in a characteristic zig-zag pattern of the iddingsite 'rods' (Figs. 4*b* and *c*). It should be stressed that intersection of the fractures with the cleavages of K-feldspar gives a similar pattern with almost the same apex angle at 75°.

On the other hand this peculiar pattern may also indicate rythmic fluctuations of the iddingsite growth rate. The shape of the 'rods' can be approximated by two opposed waves, the highest amplitude of which reflects the maximum rate of iddingsitization. The concave parts of the 'rods' may be related to the shortage in supply of oxidizing solutions. During this process fractionation of the fayalite oxidation products took place resulting in formation of silica enriched ribbons enveloped by iron hydroxide. Occasionally, the excess silica was removed from the iddingsite forming bands of shark-teeth-like layers (Fig. 4*d*). The process of alteration ended with a recrystallization of amorphous iron-hydroxide to poorly crystalline goethite.

**Acknowledgements**

I am grateful to Prof. W. S. MacKenzie for his careful and critical review of the manuscript and for improving the English of the manuscript. I am also indebted to T. Hopkins and D. Plant for their assistance in the microprobe analyses and to Dr L. Karwowski and Mrs E. Teper for their help in the fluid inclusions study. Most of this work was done while the author was on the British Council scholarship at the Department of Geology, University of Manchester.

## References

Annersten, H., Adeunji, J., and Filipides, A. (1984) *Am. Mineral.* **69,** 1110–15.

Baker, I., and Haggerty, S. E. (1967) *Contrib. Mineral. Petrol.* **16,** 258–73.

Blake, R. L. (1965) *Am. Mineral.* **50,** 148.

Deer, W. A., Howie, R., and Zussman, J. (1982) *Rock-forming minerals,* **1A,** *Orthosilicates.* (Longmans) London.

Eggleton, R. A. (1972) *Mineral. Mag.* **38,** 639–711.

——and Chappell, B. W. (1978) Ibid. **42,** 361–8.

Floran, R. J., and Papike, J. J. (1975) *Geol. Soc. Am. Bull.* **86,** 1169–90

Forbes, W. C. (1977) *Am. J. Sci.* **277,** 735–49.

Frish, T. (1972) *Can. Mineral.* **11,** 552–3.

Ginzburg, I. W., Lisitsina, G. A., Sadikova, A. T., and Sidorenko, G. A. (1961) *Trudy Min. Muzea.* **13,** 16–42.

Guggenheim, S., Bailey, S. W., Eggleton, R. A., and Wilkes, P. (1982) *Can. Mineral.* **20,** 1–18.

Janeczek, J. (1985) *Geol. Sudetica.* **20,** 2, 1–82.

Klein, C. Jr. (1974) *Can. Mineral.* **12,** 475–98.

Lenkowski, W. (1983) *Arch. Mineral.* **39,** 53–66.

Majerowicz, A. (1972) *Geol. Sudetica.* **6,** 7–96.

Miller, M. L., and Ribbe, P. H. (1985) *Am. Mineral.* **70,** 723–8.

Miyano, T., and Klein, C. (1983) Ibid. **68,** 699–716.

Nowakowski, A., and Kozłowski, A. (1983) *Arch. Mineral.* **39,** 5–16.

Puziewicz, J. (1985) *Neues Jahrb. Mineral. Abh.* **153,** 19–31.

Sachanbiński, M., and Janeczek, J. (1977) *Mineral. Polonica.* **8,** 3–14.

Wones, D. R., and Gilbert, M. C. (1969) *Am. J. Sci.* **267-A,** 480–8.

————(1982) Amphiboles in the igneous environment. In: *Amphiboles: petrology and experimental phase relations. Reviews in mineralogy,* **9B,** Mineral. Soc. America.

[*Manuscript received 22 March 1988*]